

Production of Lithium in Primordial Supernovae

Alexander Heger^{1–5} and Stan Woosley⁶

¹ School of Physics and Astronomy – Monash University, Clayton, Vic 3800, Australia

e-mail: alexander.heger@monash.edu

² Tsung-Dao Lee Institute – Shanghai 200240, China

³ Center of Excellence for Astrophysics in Three Dimensions (ASTRO-3D), Australia

⁴ OzGrav-Monash – Monash Centre for Astrophysics, School of Physics and Astronomy, Monash University, VIC 3800, Australia

⁵ Joint Institute for Nuclear Astrophysics - Center for the Evolution of the Elements (JINA-CEE), Monash University, Vic 3800, Australia

⁶ Department of Astronomy and Astrophysics – University of California at Santa Cruz, Santa Cruz, CA 95060, USA

Abstract.

The first generation of stars is quite unique. The absence of metals likely affects their formation, with current models suggesting a much more top-heavy initial mass fraction than what we observe today, and some of their other properties, such as rotation rates and binarity, are largely unknown or constrained by direct observations. But even non-rotation single stars of a given mass will evolve quite differently due to the absence of the metals: the stars will mostly remain much more compact until their death, with the hydrogen-rich later reaching down ten teens deeper in radius than in modern stars. When they explode as supernovae, the exposure to the supernova neutrino flux is much enhanced, allowing for copious production of lithium. This production will not be constant for all stars but largely vary across the mass range. Such production even more challenges the presence of the Spite Plateau.

Key words. Stars: abundances – Stars: Population III – Abundance: ⁷Li – Stars: Supernovae

1. Introduction

The tension between the clear predictions for big bang nucleosynthesis (BBN) production of ⁷Li on the one hand (Pitrou et al. 2018), and the observation of the much lower “Spite Plateau” (Spite & Spite 1982) in metal-poor or ultra-metal poor (UMP) stars persists to the present day and topic of many other contributions in these proceedings. A common explanation of the past (but see other ideas in these proceedings) has been to suggest a fixed and universal depletion/destruction process for ⁷Li from the

BBN initial abundance. In this contribution we set out to introduce an additional *production* mechanism for ⁷Li that should be present in the first generation of stars which also make the metals that are found in the stars of the Spite Plateau. This adds some extra variation in the initial ⁷Li abundance of the material of which the Spite Plateau stars have formed.

2. Massive Population III Stars

The theory of formation of Population III stars suggest that the first generation of stars has

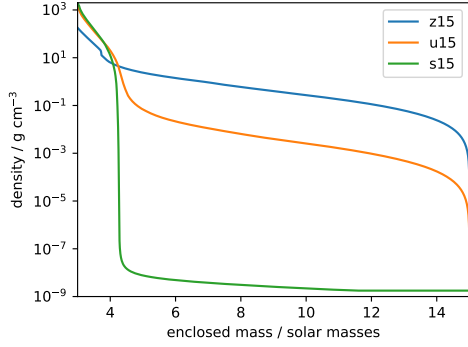


Fig. 1. Pre-supernova structure, i.e., density (y-axis) as a function of mass coordinate (x-axis), for $15 M_{\odot}$ stars of zero metallicity ($Z = 0$, z15), $[Z] = -4$ (u15), and solar metallicity ($[Z] = 0$, s15). The density in the hydrogen envelope is much higher in the Pop III model than in the ultra-metal poor (UMP) star or that of solar composition.

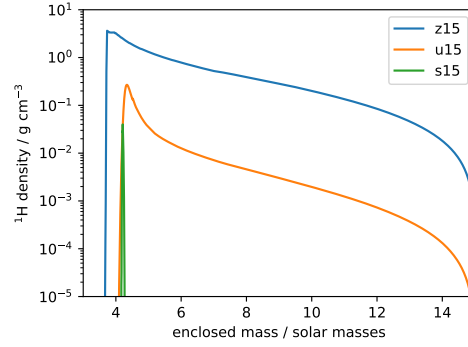


Fig. 2. Pre-supernova hydrogen density as a function of *mass* coordinate for same models as in Figure 1. The hydrogen density in the Pop III star is much higher at the base and keeps high density throughout. For the solar composition star only the very bottom mass fraction of the envelope has high hydrogen density.

been quite massive (e.g., Bromm et al. 2002; Abel et al. 2002; Hirano & Bromm 2017), with typical masses maybe in the tens to hundreds of solar masses. Understanding what the initial mass function (IMF) of the first generation of stars really is, however, remains an open question. Here we will assume they are in the massive star range.

It is this first generation of stars that make the first heavy metals in the universe, the metals that we find in the most metal-poor low-mass stars of our galaxy today. The most iron-poor star found to date only has an upper limit for its iron abundance (Keller et al. 2014; Bessell et al. 2015). To match the observed abundances, the best progenitor candidate was a $40 M_{\odot}$ star, with large fallback (Zhang et al. 2008; Chan et al. 2018), low amount of mixing (Joggerst et al. 2009), and a low dilution factor of ~ 30 for the supernova (SN) ejecta with primordial material as the initial abundance for the “Keller Star”. Remember that last number for the *Conclusions Sections*.

3. Neutrino-Induced Li Production

Based on the large compilation of non-rotating single Pop III star models and explosive yields by Heger & Woosley (2010), we assessed the

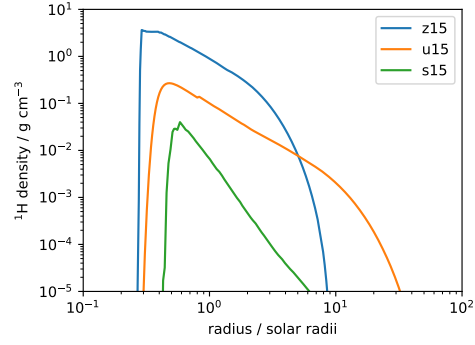


Fig. 3. Pre-supernova hydrogen density as a function of *radius* coordinate for same models as in Figure 1. The hydrogen reaches down to lower radii in the Pop III star model compared to the UMP star or solar composition.

production of ${}^7\text{Li}$ in supernovae from primordial stars. These stars uniquely lack any initial heavy elements needed for hydrogen burning by the CNO cycle. Instead, they contract until the onset of helium burning by the triple-alpha process, making a small trace of carbon, just sufficient to start the CNO cycle burning process. The same applies to hydrogen shell burning, and, as a result, the entire hydrogen shell remains quite compact and dense until the su-

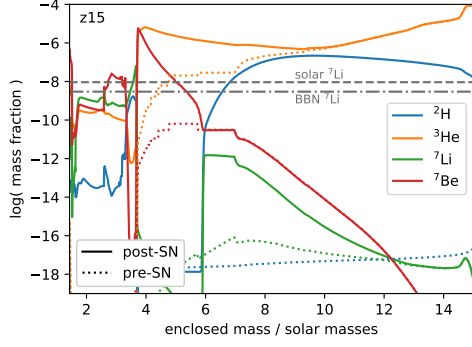


Fig. 4. Key abundances at pre-supernova stage (*dotted lines*) and 100 s after supernova explosion (*solid lines*) of a $15 M_{\odot}$ primordial star (z15) with an explosion energy of 1.2 B. ${}^7\text{Be}$ will still decay to ${}^7\text{Li}$ at a later time. We see large production of ${}^3\text{He}$ at the base of the hydrogen shell (compare to Figure 2) that burns to ${}^7\text{Be}$ at the very bottom of the hydrogen shell. The deuterium that was initially made by capture of the neutrons from neutrino interaction has all been burnt to ${}^3\text{He}$ by the SN shock wave.

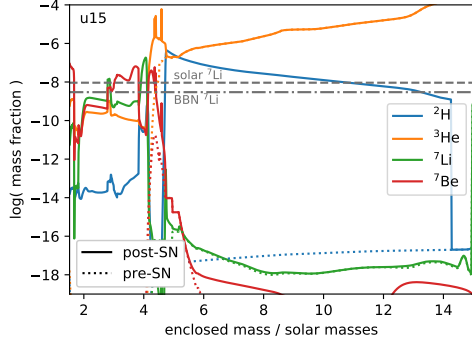


Fig. 5. Same as Figure 4 but for Model u15. There is production of ${}^2\text{H}$ but no significant production of ${}^7\text{Li}$ or ${}^7\text{Be}$ in the hydrogen envelope; there is some notable production of ${}^7\text{Be}$ from neutrino spallation in the CO core.

pernova stage as compared to more metal-rich stars (Figure 1). This leads to much higher hydrogen density in the envelope (Figure 2) and deeper into the star (Figure 3).

Unique to Pop III stars, the supernova neutrinos can now convert protons to neutrons that

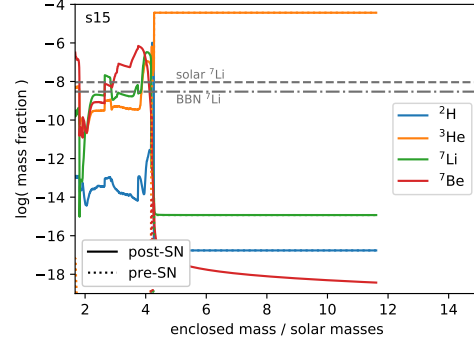


Fig. 6. Same as Figure 5 but for Model s15. There is no relevant explosive nucleosynthesis in the hydrogen envelope, but some notable production of ${}^7\text{Be}$ from neutrino spallation in the CO core similar to Model u15.

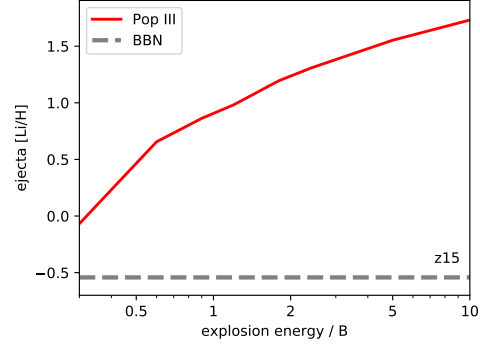


Fig. 7. Production factor $[\text{Li}/\text{H}]$ in the ejecta of a $15 M_{\odot}$ primordial star (z15) as a function of explosion energy (final kinetic energy of ejecta). The compression and heating by the explosion in the dense hydrogen envelope allows for efficient production of ${}^7\text{Li}$ by ${}^3\text{He} + {}^4\text{He} \rightarrow {}^7\text{Be}$.

uniquely react onward to make ${}^7\text{Li}$ by the reaction chain

$${}^1\text{H}(\bar{\nu}_e, e^+)n(p, \gamma){}^2\text{H}(p, \gamma){}^3\text{He}(\alpha, \gamma){}^7\text{Be}(\beta^+){}^7\text{Li},$$

leading to high production of ${}^7\text{Li}$ in the hydrogen envelope (Figure 4), that is easily ejected. In contrast, in stars of higher initial metallicity we do not find ${}^7\text{Li}$ production in the hydrogen envelope, but spallation reactions may produce ${}^7\text{Be}$ in the CO core (Banerjee et al. 2016, shown here in Figures 5 and 6). The resulting

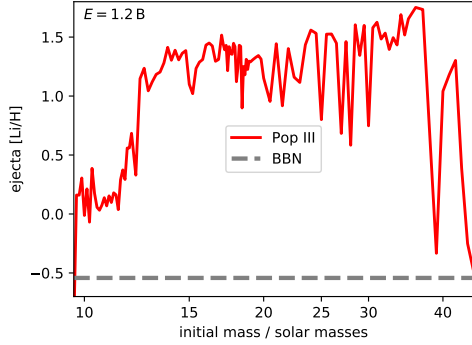


Fig. 8. Production factor $[\text{Li}/\text{H}]$ in the ejecta of a primordial stars with an explosion energy of 1.2 B as a function of initial stellar mass. For stars of higher mass fallback sets in, reducing the ${}^7\text{Li}$ yield above $40 M_{\odot}$; for higher explosion energies than the 1.2 B case shown here, however, the ${}^7\text{Li}$ production remains high.

${}^7\text{Li}$ yield in the ejecta may still be comparable to the solar abundance level.

Interestingly, the neutrino-induced neutron production alone is not the only ingredient. When the supernova shock runs through the dense hydrogen envelope, the extra heating boost the fusion reaction that lead to ${}^7\text{Li}$ production, and hence there is a sensitivity to supernova explosion energy, as shown in Figure 7. The neutrino energy and flux used to compute the neutrino-induced spallation was kept the same for all explosion energies.

4. Stellar Mass Summary

The mechanism presented here operates in supernovae; for star below the supernova mass limit it does not operate. We find about solar production from the onset of supernova explosion up to $\sim 12 M_{\odot}$ (Figure 8). We then find a plateau of Li production factor of $[\text{Li}/\text{H}] = 1.3 \dots 1.5$ from $\sim 12 M_{\odot}$ up to $\sim 45 M_{\odot}$ for explosions of $E = 1.2 B$. At higher initial mass, fallback removes the ${}^7\text{Li}$ production, but for higher explosion energies, e.g., hypernovae, high ${}^7\text{Li}$ production would persist provided the neutrino flux does not cut off, otherwise there would be little production beyond $\sim 45 M_{\odot}$.

We expect no production for very massive stars: For pulsational pair instability supernovae (PPSN) much of the hydrogen envelope would either be removed by the pulses (Woosley 2017) or the envelope would have much higher entropy and lower density due to the pulses preceding the final collapse. For higher masses, the pair instability supernovae will not make a compact remnant (Heger & Woosley 2002) and hence not produce a significant neutrino flux during the explosion (Wright et al. 2017).

As a word of further caution, the calculations presented here do not include rotation or interacting binary star evolution. Mixing processes or transfer of enriched material may reduce the ${}^7\text{Li}$ production significantly if it causes a more effective hydrogen burning by the CNO cycle, which would reduce the density of the hydrogen envelope.

5. Conclusions

Massive Pop III stars can uniquely make ${}^7\text{Li}$ by the neutrino-process due to their exceptionally compact hydrogen envelope that brings the protons closer in and to higher densities than in later generations of stars. The high densities uniquely allow for a reaction chain that leads to the production of ${}^7\text{Be}$ that later decays to ${}^7\text{Li}$. The ${}^7\text{Li}$ production is induced by charged current reaction on protons and is therefore sensitive to electron anti-neutrino energies. The interaction occurs in the hydrogen envelope outside typical neutrino oscillation density and can therefore be affected by neutrino flavour oscillations. The process is not present in pair instability supernovae (PSNe) from Pop III stars due to lack of neutrinos nor in pulsational pair instability supernovae (PPSN) due to loss of the hydrogen envelope.

If a dilution factor of ~ 30 , as derived for the Keller Star, is typical for (some) Pop III SN, the production can be well above big bang nucleosynthesis for top-heavy initial mass functions (IMF) of Pop III stars, as is often assumed. This would result in variations of the initial ${}^7\text{Li}$ abundances of second generations stars such as the Keller star by a factor 2 or more. It would make it difficult to explain

the flatness of the Spite plateau by some destruction mechanism acting on the BBN ${}^7\text{Li}$ abundances at an about constant efficiency. The origin of ${}^7\text{Li}$ abundances in the Spite Plateau would have to be of a different nature.

Observations of ${}^7\text{Li}$ variations in second-generation initial abundances may provide important constraints on many properties of Pop III stars, such as internal mixing processes, rotation rates, or their initial mass function.

Acknowledgements. This project has been supported by a grant from Science and Technology Commission of Shanghai Municipality (Grants No.16DZ2260200) and National Natural Science Foundation of China (Grants No.11655002). Parts of this research were supported by the Australian Research Council Centre of Excellence for All Sky Astrophysics in 3 Dimensions (ASTRO 3D), through project number CE170100013. Parts of this research were conducted by the Australian Research Council Centre of Excellence for Gravitational Wave Discovery (OzGrav), through project number CE170100004. This work was supported in part by the National Science Foundation under Grant No. PHY-1430152 (JINA Center for the Evolution of the Elements).

References

- Abel, T., Bryan, G. L., & Norman, M. L. 2002, *Science*, 295, 93
- Banerjee, P., Qian, Y.-Z., Heger, A., & Haxton, W. 2016, in *European Physical Journal Web of Conferences*, Vol. 109, European Physical Journal Web of Conferences, 06001
- Bessell, M. S., Collet, R., Keller, S. C., et al. 2015, *ApJ*, 806, L16
- Bromm, V., Coppi, P. S., & Larson, R. B. 2002, *ApJ*, 564, 23
- Chan, C., Müller, B., Heger, A., Pakmor, R., & Springel, V. 2018, *ApJ*, 852, L19
- Heger, A. & Woosley, S. E. 2002, *ApJ*, 567, 532
- Heger, A. & Woosley, S. E. 2010, *ApJ*, 724, 341
- Hirano, S. & Bromm, V. 2017, *MNRAS*, 470, 898
- Joggerst, C. C., Woosley, S. E., & Heger, A. 2009, *ApJ*, 693, 1780
- Keller, S. C., Bessell, M. S., Frebel, A., et al. 2014, *Nature*, 506, 463
- Pitrou, C., Coc, A., Uzan, J.-P., & Vangioni, E. 2018, *Phys. Rep.*, 754, 1
- Spite, F. & Spite, M. 1982, *A&A*, 115, 357
- Woosley, S. E. 2017, *ApJ*, 836, 244
- Wright, W. P., Gilmer, M. S., Fröhlich, C., & Kneller, J. P. 2017, *Phys. Rev. D*, 96, 103008
- Zhang, W., Woosley, S. E., & Heger, A. 2008, *ApJ*, 679, 639